Inorganic Chemistry Communications 49 (2014) 19–23

Contents lists available at ScienceDirect

Inorganic Chemistry Communications

journal homepage: www.elsevier.com/locate/inoche

A 3-fold interpenetrating 3D Cu(II) coordination polymer based on a semi-rigid naphthalene-based bis-pyridyl-bis-amide and thiophene-2,5-dicarboxylate

Xiuli Wang *, Mao Le, Hongyan Lin, Jian Luan, Guocheng Liu, Juwen Zhang, Aixiang Tian

Department of Chemistry, Bohai University, Liaoning Province Silicon Materials Engineering Technology Research Centre, Jinzhou 121000, PR China

ARTICLE INFO

Article history:
Received 10 July 2014
Received in revised form 3 September 2014
Accepted 9 September 2014
Available online 10 September 2014

Keywords:
Coordination polymer
Interpenetrating network
Semi-rigid bis-pyridyl-bis-amide ligand
Fluorescent property
Selective photocatalysis

ABSTRACT

A new 3D Cu(II) coordination polymer $[Cu_2(4\text{-dpna})_2(2,5\text{-tdca})_2]$ (**1**) (4-dpna = N^1,N^4-di(pyridin-4-yl)naphthalene-1,4-dicarboxamide, 2,5-H_2tdca = thiophene-2,5-dicarboxylic acid) has been hydrothermally synthesized. Complex **1** is a novel 3D metal–organic coordination complex based on a semi-rigid naphthalene-based bis-pyridyl-bis-amide ligand, which shows a 3-fold interpenetrating network with a $CdSO_4$-like topology. Moreover, the fluorescent property, electrochemical behavior and selective photocatalytic activity of **1** have been investigated.

In recent years, the investigation of coordination polymers (CPs) with interpenetrating features has made considerable progress in the fields of crystal engineering, owing to their intriguing architectures [1] and potential applications as multifunctional materials [2]. Until now, many CPs with interpenetrating structures have been prepared and comprehensively discussed, such as 2-, 3-, 4-, 8- and even 25-fold interpenetrating networks [3]. However, the rational design and construction of interpenetrating networks are still big challenges since a lot of factors may influence the final structures of CPs, such as the coordination geometry of metal ions, organic ligands, reactants ratio, pH value, solvents, and temperature [4]. Among these factors, the introduction of the long organic ligands containing appropriate coordination sites could be very helpful in building high-dimensional structures with large channels, which may be conducive to form interpenetrating networks [4a]. For example, by choosing a flexible bis-pyridyl-bis-amide ligand, Chen and co-workers have synthesized a 12-fold interpenetrating diamondoid network $[CuSO_4(L)(H_2O)_2]_\infty$ (L = *N*,*N*′-di(4-pyridyl)adipoamide) [4c]. By introducing the same ligand L into the metal–dicarboxylate system, Chen's group has prepared two interpenetrated diamondoid networks $\{[Zn(L)(1,4\text{-BDC})]\cdot H_2O\}_n$ and $\{[Cd(L)(1,4\text{-BDC})]\cdot 2H_2O\}_n$ (1,4-H_2BDC = 1,4-benzenedicarboxylic acid), which show distorted cages with 8- and 9-fold interpenetrating modes [4f]. Based on the semi-rigid bis-pyridyl-bis-amide *N*,*N*′-bis(4-pyridinecarboxamide)-1,4-benzene (3-bpcb) and 1,3,5-benzenetricarboxylic acid (1,3,5-H_3BTC) mixed ligands, our group firstly obtained a 3D complex $[Cu_3(3\text{-bpcb})_3(BTC)_2]_3\cdot\sim 12H_2O$, in which discrete $(H_2O)_{12}$ clusters are dispersed in the 3-fold interpenetrating 3D network [5]. In this regard, the long bis-pyridyl-bis-amide ligands have proven to be excellent N-donor ligands for building CPs containing large channels or pores, which may help to construct interpenetrating networks.

Pursuing our previous study in this area, we introduce a semi-rigid naphthalene-bridging group into the bis-pyridyl-bis-amide organic ligand and obtain the long semi-rigid ligand N^1,N^4-di(pyridin-4-yl)naphthalene-1,4-dicarboxamide (4-dpna) (Scheme 1), which is employed as the main ligand in this work based on the following considerations: (i) its pyridyl and amide groups can provide more potential coordination sites; (ii) its two amide groups may be potential hydrogen bonding sites; and (iii) its naphthalene-based spacer has larger steric hindrance and may conduce to constructing the networks with big voids. The $CuCl_2\cdot 2H_2O$, 4-dpna and thiophene-2,5-dicarboxylic acid (2,5-H_2tdca) were selected as starting materials and reacted under the hydrothermal condition, with the expectation to get high-dimensional interpenetrating network. Fortunately, a new coordination polymer showing a 3-fold interpenetrating 3D network with a $CdSO_4$-like topology, $[Cu_2(4\text{-dpna})_2(2,5\text{-tdca})_2]$ (**1**), was obtained. To the best of our knowledge, it represents the first example of interpenetrating complex with a semi-rigid naphthalene-based bis-pyridyl-bis-amide ligand. The syntheses, structures, and properties of the title complex were investigated in detail.

The 4-dpna ligand was prepared according to the literature method [6]. Complex **1** was obtained by the hydrothermal reaction of

* Corresponding author.
E-mail address: wangxiuli@bhu.edu.cn (X. Wang).

http://dx.doi.org/10.1016/j.inoche.2014.09.011
1387-7003/

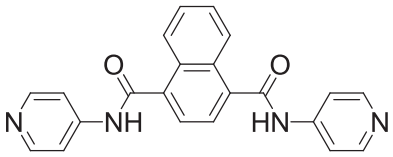

4-dpna

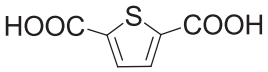

2,5-H_2tdca

Scheme 1. The bis-pyridyl-bis-amide 4-dpna and dicarboxylic acid 2,5-H_2tdca.

$CuCl_2 \cdot 2H_2O$, 4-dpna, 2,5-H_2tdca, and H_2O at 150 °C for 4 days [7]. Single crystal X-ray diffraction analysis [8] reveals that the asymmetric unit of complex **1** contains three crystallographically independent Cu(II) ions (Cu1, Cu2 and Cu3) (Fig. 1). Each Cu(II) ion is four-coordinated by two pyridyl N atoms from two different 4-dpna ligands and two carboxyl O atoms from two different 2,5-tdca anions in a quadrilateral style. The bond distances and angles around Cu(II) ions are 1.993(2)–2.048(2) Å for Cu – N, 1.908(2)–1.985(2) Å for Cu – O, 158.90(1)–180° for N – Cu – N, 88.94(1)–96.60(1)° for N – Cu – O, and 161.38(1)–180° for O – Cu – O.

In complex **1**, the 4-dpna ligand adopts only one μ_2-bridging coordination mode, but it displays two types of conformations (modes A and B, Table S3): (i) It connects two Cu(II) ions with the non-bonding Cu1 – Cu3 distance of 19.50 Å (mode A), and the corresponding dihedral angle between the pyridyl rings is 81.14°; and (ii) it connects Cu2 and Cu3 with the non-bonding distance of 19.65 Å (mode B), in which the dihedral angle between the two pyridyl ring is 8.26°. Thus, the two types of 4-dpna ligands alternately link the Cu(II) ions to form a 1D $[Cu(4\text{-dpna})]_n$ *meso*-helical chain, in which the long helical pitch is 78.30 Å (Figs. 2b, S1). To the best of our knowledge, it is the longest helical pitch in the helical chains derived from the bis-pyridyl-bis-amide ligands [4c,f]. Furthermore, the adjacent Cu1 and Cu2 ions are alternately connected by 2,5-tdca anions to form a 1D $[Cu(2,5\text{-tdca})]_n$ infinite chain with the Cu1 – Cu2 distance of 10.40 Å (Figs. 2a, S1). Ultimately, the $[Cu(4\text{-dpna})]_n$ helixes and $[Cu(2,5\text{-tdca})]_n$ infinite chains construct a 3D coordination framework by sharing Cu(II) ions (Fig. 2c). It is interesting that there exist two types of cavities (big A and small B) in the 3D framework (Fig. 2c). For cavities A, the naphthalene groups of 4-dpna ligands are located outside of the cavities; while for cavities B, the naphthalene groups of 4-dpna ligands are located in the inside of the cavities, and there are weak π–π stacking interactions among the naphthalene groups of 4-dpna ligands [values of the shortest centroid–centroid distance of 4.7074 Å].

If the Cu(II) ion is considered as 4-connected node, 4-dpna ligand and 2,5-tdca anions are considered as two kinds of linkers, the structure of **1** is a 4-connected distorted $CdSO_4$-like topology (Fig. S2). The large cage (39.55 × 40.54 $Å^2$ for A) in complex **1** induces the formation of interpenetrating framework to stabilize the whole structure. Three same 3D frameworks interpenetrate with each other and lead to form an interesting 3-fold interpenetrating structure (Fig. 3).

The IR spectra of complex **1** are shown in Fig. S3. The strong peaks at 1371 and 1050 cm^{-1} suggest the ν_{C-N} stretching vibrations of the pyridyl ring of the 4-dpna ligand [9]. The presence of the characteristic bands at 1619 and 1423 cm^{-1} may be attributed to the asymmetric and symmetric vibrations of carboxyl groups [10]. The presence of the characteristic band at 1664 cm^{-1} is identified $\nu_{C=O}$ vibrations of the amide groups [9,10].

The thermogravimetric (TG) analysis was performed under N_2 atmosphere with a heating rate of 10 °C min^{-1} in the range of 20 to 790 °C, as shown in Fig. S4. The TG curve of complex **1** shows only one weight loss step, and the organic components in **1** decompose from 325 to 400 °C. The remaining residue corresponds to the formation of CuO (obsd. 13.25%, calcd. 13.20%).

The solid state fluorescent property of complex **1**, together with the free 4-dpna ligand, was investigated at room temperature (Fig. S5). The free ligand 4-dpna exhibits the emission peak at 400 nm with the excitation at 320 nm, which may be assigned to the $\pi^* \rightarrow \pi$ transitions [11]. The ligand 2,5-H_2tdca shows very weak π^*–n transitions and contributes a little to the fluorescence of the title complex at room temperature [12]. Despite Cu(II) complexes do not contain d^{10} metal centers, a series of fluorescent Cu(II) complexes have been reported [13]. Density functional theory calculation indicates that the fluorescence of Cu(II) complexes may be attributed to the coupling of ligand-based emission and ligand-to-metal charge-transfer (LMCT) [13–15]. Upon the same excitation, the emission peak of complex **1** is at 396 nm. Compared with the free 4-dpna ligand, a slight red-shift of 4 nm for the emission band of complex **1** has been observed. Therefore, the fluorescence behavior of the title complex may be best assigned to the LMCT [14,15].

The electrochemical behavior of complex **1** bulk-modified carbon paste electrode (**1**-CPE) was carried out in 0.01 M H_2SO_4 + 0.5 M Na_2SO_4 aqueous solution. It can be seen clearly that a quasi-reversible redox peak is observed at the **1**-CPE in the potential range of 300 to −300 mV, which could be attributed to the redox couple of Cu(II)/Cu(I) (Fig. 4) [16]. The mean peak potential $E_{1/2} = (E_{pa} + E_{pc}) / 2$ is −35 mV for **1**-CPE. As shown in Fig. 4, with the scan rates increasing from 20 to 200 mV s^{-1}, the peak potential of the **1**-CPE changes gradually: the cathodic peak potentials shift to the negative direction, and the corresponding anodic peak potentials shift to the positive direction. The plots of peak currents versus scan rates were shown in the inset of Fig. 4. The anodic and cathodic peak currents were proportional to the scan

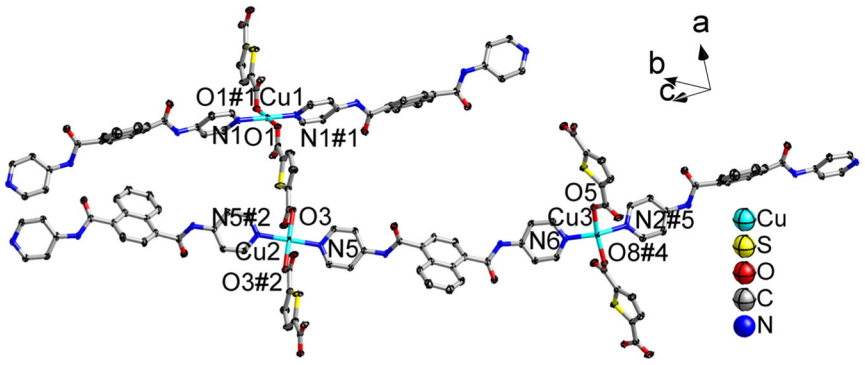

Fig. 1. The coordination environment of the Cu(II) ions in **1**. All of the hydrogen atoms have been omitted for clarity (symmetry code: #1 $-x, -y+1, -z+1$; #2 $-x-1, -y, -z+2$; #4 $x-1, y, z$; #5 $x, y-2, z-1$).